Eradication-resolution dynamics with stochastic flare-ups

Hugo A. van den Berg[a,*], Zoe A. Duncombe[a]

[a]*Mathematics Institute, University of Warwick, Coventry CV4 7AL UK*

Abstract

In infectious disease as well as in cancer, the ultimate outcome of the curative response, mediated by the body itself or through drug treatment, is either successful eradication or a resurgence of the disease ("flare-up" or "relapse"), depending on random fluctuations that dominate the dynamics of the system when the number of diseased cells has become very low. The presence of a low-numbers bottle-neck in the dynamics, which is unavoidable if eradication is to take place at all, renders at least one phase of the dynamics essentially stochastic. However, the eradicating agents (e.g. immune cells, drug molecules) generally remain at high numbers during the critical bottle-neck phase, sufficiently so to warrant a deterministic treatment. This leads us to consider a hybrid stochastic-deterministic approach where the infected cells are treated stochastically whereas the eradicating agents are treated deterministically. Exploiting the fact that the number of eradicating agents typically decreases monotonically during the resolution phase of the response, we derive a set of coupled first-order differential equations that describe the probability of ultimate eradication as a function of the system's state, and we consider a number of biomedical applications.

Keywords: Cancer, Infection, Eradication, Extinction bottleneck, T cells, Stochastic processes

1. Introduction

Eradication-resolution dynamics occurs whenever a proliferative disease is being cleared by an agent that is diminishing in numbers. For example, in cancer therapy with immunostimulatory monoclonal antibodies, the antibodies mediate a connection between tumour cells and immune effector cells, and are thus destroyed as the cancer is being eradicated (Bargou et al. (2008); Hudis (2007); Melero et al. (2007)), whereas in a T cell response against a viral infection, the number of T cells drops as the infection is being eradicated (Badovinac et al. (2002), Van den Berg and Kiselev (2004); Harty and Badovinac (2008)). Such eradication-resolution processes are characterised by a dichotomy of outcomes: the disease may be successfully eradicated, or it might escape, "flaring up" after an initial decrease. This behaviour is illustrated qualitatively in Fig. 1. Starting with a sufficient dosage of the anti-cancer drug, the tumour size initially drops and then increases again as the amount of drug remaining in the system steadily falls (Bargou et al. (2008)). On a deterministic treatment of the problem, the ultimate outcome is always a relapse of the cancer following a temporary remission (Fig. 1, left panel; equations are given below in Section 3.2). For some trajectories, the size of the tumour passes through a minimum that corresponds to just a few cells (or even less than one cell; this is the infamous "attofox" effect). Clearly, the deterministic treatment breaks down at low numbers of tumour cells. Moreover, whether eradication occurs or not depends critically on stochastic effects.

*Corresponding author
Email address: hugo@maths.warwick.ac.uk (Hugo A. van den Berg)

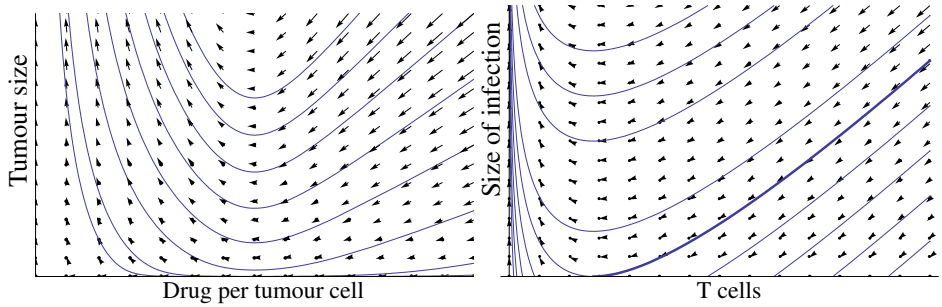

Figure 1: Phase portraits of deterministic examples of eradication-resolution dynamics.

A slightly more complex example is shown in the right panel of Fig. 1 (equations are given and discussed in Section 3.3). Here, both outcomes are possible even in a deterministic treatment: the phase plane is divided into two regions, one in which ultimate eradication is certain and one in which ultimate flare-up is certain. The regions are separated by a critical trajectory which serves as separatrix (the heavy line in Fig. 1). Again, stochastic fluctuations become important as the number of infected cells approaches low numbers, and the probability of eradication would not be expected to jump crisply from 0 to 1 at the deterministic separatrix.

In both examples, it appears that the appropriate approach is to associate with each point in the phase plane the probability that a stochastic trajectory starting at this point will result in eradication. This is a problem of immediate medical interest: when confronted with a tumour mass of a given size, the clinician wants to know the minimal dose that corresponds to a pre-determined likelihood of success. Thus, the evaluation of eradication probabilities from the extent of the disease and a proposed dosage of eradicating agent is central to rational design of treatment.

More realistic deterministic models of tumour growth (including e.g. spatial effects of diffusion limitation and vascularization), its induced immune response (including e.g. delays in response and clonal expansion), and medical treatment (which may act directly or via immune manupulation) exhibit a richer range of dynamic behaviours (e.g. Araujo and McElwain (2004); de Pillis et al. (2005); Sachs and Hlatky (2010)). Of concern here is the ultimate behaviour of such dynamics, which may be a non-zero equilibrium for the tumour, or some sort of cycling behaviour. In the latter case, the upstrokes of the cycling may be viewed as flare-ups, or the amplitude of the cycle may be small enough that the behaviour is best regarded as oscillations about a non-zero value. But then, from a stochastic point of view, either eradication or flare-up will still be almost certain to occur at some point in time. Of course, as the tumour equilibrium size increases, the probability that either eradication or flare-up occurs during the lifetime of the subject becomes vanishingly small, and thus the need to incorporate a stochastic treatment disappears as well. It is with these caveats in mind that tumour dynamics is regarded as an instance of eradication-resolution dynamics with two possible eventual outcomes.

This paper considers the stochastic treatment of eradication-resolution dynamics and, in particular, the calculation of the eradication probability as a function of initial conditions. The method outlined in Section 2 exploits a typical feature of eradication-resolution systems, viz. that the stochasticity near the point of eradication is almost entirely due to the disease component (cancer cells, infected cells, virions etc.), while the eliminating agents (antibodies, drug molecules, T cells etc.) remain present at numbers that warrant a mean-field approach. This motivates a hybrid stochastic-deterministic dynamical system, where the low-

numbers component is treated stochastically and the high-numbers component is treated deterministically. The approach is illustrated in the case of a number of typical biological examples in Section 3. A natural extension is considered in Section 4.

2. Eradication probability flow

Deterministic eradication-resolution dynamics can be represented in a fairly general setting by the following system of ordinary differential equations:

$$\frac{d}{dt}x = -\mu g(x,N)x \tag{1}$$

$$\frac{d}{dt}N = \rho h(x,N)N - \vartheta f(x,N)x \tag{2}$$

where x is the eradicating agent, N is the number of pathogenic entities, μ, ρ, and ϑ are positive parameters, and g, h, and f are "functional response" functions, dimensionless multipliers taking values in the interval $[0,1]$, with the stipulation that $g(x,N) \neq 0$ whenever $N > 0$; thus μ, ρ, and ϑ are maximum specific rates of, respectively, agent decay, disease spreading, and eradication. A pair $(x(t),N(t))$ is called an *eradication solution* if it satisfies equations (1) and (2) and $N(t) \to 0$ as $t \to \infty$, whereas $(x(t),N(t))$ is a *flare-up solution* if it satisfies equations (1) and (2) and $\lim_{t\to\infty} N(t) > 0$.

On the deterministic approach, x and N are both non-negative real numbers. However, since eradication requires that N pass at least once through a stage where $N \sim 1$, a deterministic treatment is not justified. Also, the deterministic system may not even admit an eradication solution. Accordingly, equation (2) is replaced by a continuous-time Markov chain, with $N \in \{0,1,2,\dots\}$ and event rate $\rho h(x,N)N + \vartheta f(x,N)x$ for increment/decrement events ($N \to N \pm 1$). The problem is to characterise the function $P_N(x)$, which is the probability of ultimate eradication if the system is started in the state (x,N). The eradication function is determined by the dynamics together with the following boundary conditions:

$$P_0(x) = 1 \quad \text{for } x \geq 0\,; \tag{3}$$

$$P_N(0) = 0 \quad \text{for } N \geq 1\,. \tag{4}$$

It is assumed that the agent variable x corresponds to a sufficiently large number of entities to warrant a deterministic treatment (this may not be strictly valid for flare-up solutions in which x tends to zero as $t \to \infty$; however, the behaviour of x in such cases is not qualitatively important, since N will have passed its low-numbers bottle-neck in the long-time limit).

Let $z = x^{-1}$ and $P(z,N) \equiv P_N(x)$, so that

$$\frac{d}{dt}z = \mu g(z^{-1},N)z \tag{5}$$

By the above assumptions, for fixed positive N, z is a monotone increasing function of t, which allows us to use replace t in the continuous-time Markov chain by z. Noting that

$$\begin{aligned}
&\mathbb{P}\{N \text{ remains constant during an interval of duration } \delta t\} \\
&\quad = \exp\{-(\rho h(z^{-1},N)N + \vartheta f(z^{-1},N)z^{-1})\delta t\} \\
&\quad \doteq 1 - (\rho h(z^{-1},N)N + \vartheta f(z^{-1},N)z^{-1})\delta t \\
&\quad \doteq 1 - \frac{\rho h(z^{-1},N)N + \vartheta f(z^{-1},N)z^{-1}}{\mu g(z^{-1},N)z}\delta z
\end{aligned} \tag{6}$$

we have, by a straightforward application of the law of total probability,

$$P(z,N) \doteq \left(1 - \frac{\rho h(z^{-1},N)N + \vartheta f(z^{-1},N)z^{-1}}{\mu g(z^{-1},N)z}\delta z\right) P(z+\delta z,N) + \left(\frac{\rho h(z^{-1},N)N}{\mu g(z^{-1},N)z} P(z+\delta z,N+1) + \frac{\vartheta f(z^{-1},N)z^{-1}}{\mu g(z^{-1},N)z} P(z+\delta z,N-1)\right)\delta z \quad (7)$$

for $N \geq 1$. Rearranging this probability conservation law, taking the limit

$$\frac{dP(z,N)}{dz} = \lim_{\delta z \to 0} \frac{P(z+\delta z,N) - P(z,N)}{\delta z} \quad (8)$$

and transforming back, we obtain a system of ordinary differential equations for the probability flow:

$$\frac{dP_N(x)}{dx} = \frac{\rho h(x,N)N + \vartheta f(x,N)x}{\mu g(x,N)x}\left(p_{\text{up}} P_{N+1}(x) + (1-p_{\text{up}})P_{N-1}(x) - P_N(x)\right) \quad (9)$$

with

$$p_{\text{up}} = \frac{\rho h(x,N)N}{\rho h(x,N)N + \vartheta f(x,N)x} \quad (10)$$

for $N \geq 1$.

One solution is $P_N(x) \equiv 1$ for $x > 0$ and $N \geq 1$, i.e. eradication is certain from all starting positions. This would require a jump discontinuity at the N-axis, since $P_N(0) = 0$ for $N \geq 1$. To decide whether this is admissible, we must consider the behaviour near the N-axis more carefully. The essential difficulty is that the justification for a deterministic treatment in the x-direction breaks down near the N-axis. Consider momentarily a fully stochastic treatment, in which x is replaced by a discrete variable $X \in \mathbb{N}$. For $X = 1$ and $N \geq 1$, the law of total probability then gives the following equation:

$$P_N(1) = \frac{\rho hN P_{N+1}(1) + \mu g P_N(0) + \vartheta f P_{N-1}(1)}{\rho hN + \mu g + \vartheta f} \quad (11)$$

(with a slight abuse of notation since X, which is absolute-scaled, has replaced ratio-scaled x). Since $g > 0$ at $X = 1$ by assumption and $P_N(0) = 0$, $P_N(1)$ is strictly smaller than 1, which rules out the solution $P_N(x) \equiv 1$. This accords with the intuitive expectation that for small x, the probability of eradication decays quickly to zero with increasing N. This argument motivates the following approximate boundary condition for the system with real x:

$$P_N(\delta x) \equiv 0 \quad \text{for } N \geq 1 \quad (12)$$

for some small value $\delta x > 0$. Heuristically, we can think of δx as a boundary width satisfying the requirement that the deterministic treatment of x is admissible for $x > \delta x$. Since trajectories that enter the strip

$$\{(x,N) \mid 0 < x < \delta x\ ,\ N \geq 0\}$$

cannot leave it, the fact that the ultimate fate of the eradicating agent is discrete absorption, rather than asymptotic decay, does not materially affect the eradication analysis.

To obtain numerical solutions, two truncations are required. The first is the approximate boundary condition (12). Secondly, only finitely many (say $\widehat{N}$) equations can be evaluated, prompting the replacement of $P_{\widehat{N}+1}(x)$ by $P_{\widehat{N}}(x)$ in equation (9), which gives:

$$\frac{dP_{\widehat{N}}(x)}{dx} = \frac{\vartheta f(x,\widehat{N})}{\mu g(x,\widehat{N})}\left(P_{\widehat{N}-1}(x) - P_{\widehat{N}}(x)\right)\ . \quad (13)$$

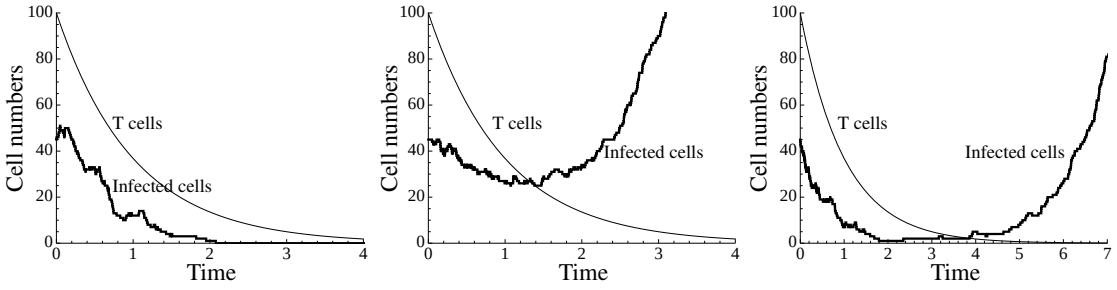

Figure 2: Simulated time courses of the hybrid stochastic-deterministic system derived from eqns (17) and (18), with $K = 5$ and $\mu = 1$. The thin line depicts the deterministic dynamics of the T cells (x) and the thick line depicts the stochastic dynamics of the number of infected cells (N).

Numerical solutions must be checked against an unwarranted influence of the chosen values for δx and $\widehat{N}$.

The general form of equation (9) is

$$\dot{\mathbf{x}} \cdot \nabla P_{\mathbf{N}}(\mathbf{x}) = \sum_{\Delta \mathbf{N}} h_{\Delta \mathbf{N}}(\mathbf{x}, \mathbf{N}) \left(P_{\mathbf{N}}(\mathbf{x}) - P_{\mathbf{N}+\Delta \mathbf{N}}(\mathbf{x}) \right) \tag{14}$$

where $\mathbf{x}$ is the deterministic component of the state, evolving with dynamics $\dot{\mathbf{x}}$, and $\mathbf{N}$ is the stochastic component, capable of elementary transitions $\Delta \mathbf{N}$ which occur with hazard rates denoted as $h_{\Delta \mathbf{N}}$. This is not in every case the most convenient form of the master equation, but it proves to be useful in eradication-decay dynamics where both components are scalar and (as in the examples of Section 3) $\dot{x}$ is negative everywhere.

3. Applications

We consider various specifications of the general equations, along with biological interpretations. Each example is designed to illustrate a feature of the present approach.

3.1. Eradication of an intracellular infection by T cells

The first example is defined by the following specifications:

$$g \equiv 1 \quad h \equiv 1 \quad f = \frac{N}{K+N}$$

where K is a positive parameter. Thus

$$\frac{d}{dt}x = -\mu x \tag{15}$$

$$\frac{d}{dt}N = \rho N - \vartheta \frac{N}{K+N} x \tag{16}$$

Biologically, this system may be interpreted as follows: N denotes the number of cells that have been infected with an intracellular pathogen such as a virus. The proliferation of the infection, at specific rate ρ, is stemmed by the action of T cells which bear a receptor that is specific to a molecular characteristic of the pathogen.

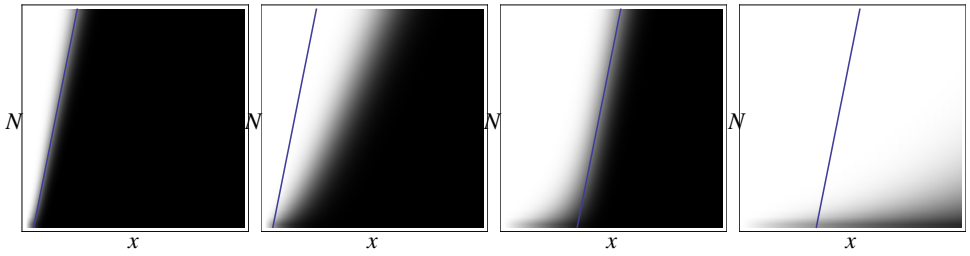

Figure 3: $P_N(x)$ for the simple T cell example (white: probability 0; black: probability 1; grey: probability in interval $(0,1)$). Abscissa is $0 < x \leq 150$, ordinate is $1 \leq N \leq 30$. Far left: $K = 5$, $\mu = 0.001$; middle left: $K = 5$, $\mu = 1$; middle right: $K = 50$, $\mu = 0.001$; far right: $K = 50$, $\mu = 1$. The heavy line is the deterministic null isocline for N.

In this model, the T cells have a standard hyperbolic functional response (Van den Berg and Kiselev (2004)) and decay autonomously and exponentially during the so-called *contraction phase* (Badovinac et al. (2002)). Two parameters can be eliminated by scaling:

$$\frac{d}{dt}x = -\mu x \tag{17}$$

$$\frac{d}{dt}N = N - \frac{N}{K+N}x \tag{18}$$

(deterministically, K could be eliminated as well, but this is not possible for the stochastic treatment since N is expressed on an absolute scale).

Hybrid stochastic-deterministic dynamics are obtained by replacing the equation for N by stochastic dynamics as outlined in Section 2; typical simulation results are shown in Fig 2. If N has the value $N_1 > 0$ on time t_1, the probability that the first step change in N (either to $N_1 + 1$ or $N_1 - 1$) will occur at a time greater than $t_1 + \tau$ is given by:

$$\exp\left\{-N_1\tau - \frac{x_0 N_1 \exp\{-\mu t_1\}}{\mu\,(K+N_1)}\,(1-\exp\{-\mu\tau\})\right\}$$

(which is obtained by integrating the hazard rate $N_1\,(1+x(t)/(K+N_1))$ where $x(t) = x_0\exp\{-\mu t\}$, the solution of eqn (17)). Starting from the same initial conditions, the outcome can be eradication or flare-up (Fig. 2, left and middle panels): the variable N may spend some time in the low-numbers bottle-neck before the flare-up takes off (Fig. 2, right panel).

Numerical solution of the probability flow equations for $P_N(x)$ is straightforward. Representative solutions are shown in Fig. 3. When the T cell numbers decay slowly and the saturation parameter K is low, the probability of eradication rises quickly from zero to 1 as x crosses the deterministic null isocline of N. Fast T cell decay means that the probability of eradication is virtually zero in the neighbourhood of the deterministic null isocline of N, and greater T cell numbers are needed to obtain a reasonable probability of eradication. Larger K-values have the effect of blurring somewhat the change-over from low to high probability near the N-null isocline.

The ability to achieve $P_N(x)$ near 1 for T cell numbers that sufficiently large given the prevailing size of the infection, especially at low T cell decay rates, lends credibility to the hypothesis that T cell expansion

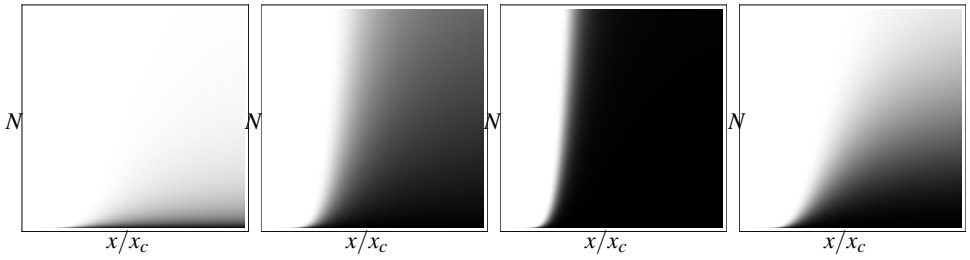

Figure 4: $P_N(x)$ for the cancer example (white: probability 0; black: probability 1; grey: probability in interval $(0,1)$). Abscissa is $0 < x/x_c \leq 5$, ordinate is $1 \leq N \leq 1500$; $K = 50$; $\eta = 5$. Far left: $\mu K/\rho = 100$, $\vartheta/\rho = 15$; middle left: $\mu K/\rho = 50$, $\vartheta/\rho = 15$; middle right: $\mu K/\rho = 25$, $\vartheta/\rho = 15$; far right: $\mu K/\rho = 25$, $\vartheta/\rho = 10$.

and contraction follows a stereotypical or "programmed" response pattern (Badovinac and Harty (2006)): provided the initial expansion delivers a clonal size $x_0 \gg K + N_0$ where N_0 is the size of the infection at the onset of the contraction phase, eradication is virtually assured. Against this hypothesis of programmed contraction, one could point to the possibility of a delayed flare-up after the T cells have decayed deterministically during the low-numbers phase and argue for the hypothesis of regulated contraction, which states that the rate of T cell decay depends, at each moment in time, on the value of N at that point in time; see Section 3.3, as well as Van den Berg and Kiselev (2004) for arguments in favour of regulated contraction.

3.2. Elimination of a tumour by immunostimulatory antibodies

Consider a tumour, proliferating at specific rate $\rho > 0$ and let Y denote the molar amount of drug active in the body. The drug is a monoclonal antibody that binds to the surface of the cancer cells, being specific to tumour-specific surface antigens; the Fc tail of the drug molecule binds to the surface of an immune effector cell which kills the cancer cell (Hudis (2007)); alternatively, the drug is a fusion molecule which can engage immune cells that lack the Fcγ receptor, such as T cells (Löffler et al. (2000)). For the sake of simplicity, we consider eradication-resolution dynamics for the scenario in which a single dose is administered, and we ignore a multiple dosage or drug infusion regime of administration, which may also be clinically relevant.

Assume that the drug partitions between cancer cells and a fluid phase (blood plasma, tissue fluid) so that a fraction $N/(N+K)$ is bound, where K is a binding constant. The amount of drug bound per cell may then be defined as follows:

$$x = \frac{Y}{N+K} \,. \tag{19}$$

The effectiveness of the drug is assumed to be a sigmoid increasing function of x:

$$\frac{d}{dt}N = \rho N - \vartheta \frac{N}{1+(x/x_c)^{-\eta}} \tag{20}$$

where $\vartheta > \rho$ is the maximum killing rate per tumour cell and x_c and η are positive parameters that determine the shape of the drug effectiveness curve. Drug molecules are assumed to be destroyed when they are bound to a cell that is being destroyed, whereas the free drug molecules disappear with rate $\mu \geq 0$, thus:

$$\frac{d}{dt}Y = -\vartheta \frac{N}{1+(x/x_c)^{-\eta}} x - \mu \frac{KY}{K+N} \,. \tag{21}$$

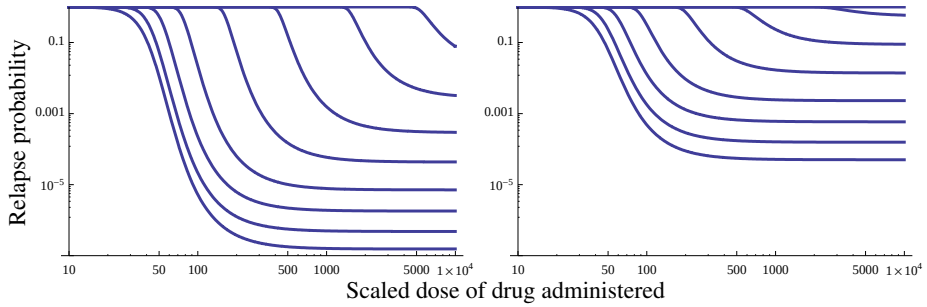

Figure 5: Relapse probability $1-P_N(x)$ as a function of scaled drug dose Y/x_c; $K=50$; $\mu K/\rho=25$; $\eta=5$. Left: $\vartheta/\rho=10$; right: $\vartheta/\rho=15$. In each panel curves are for (top to bottom): $N=3000$, 1000, 300, 100, 30, 10, 3, 1.

From equations (20) and (21) we can derive the deterministic component of the eradication-resolution dynamics:

$$\frac{d}{dt}x=-\mu\frac{K+(\rho/\mu)N}{K+N}x\,. \tag{22}$$

The stochastic component is defined by the event rate

$$\left(\rho+\frac{\vartheta}{1+(x/x_c)^{-\eta}}\right)N$$

and the probability for the event $N\to N+1$ is given by:

$$p_{\rm up}=\left(1+(\vartheta\rho)\,(x/x_c)^{-\eta}\right)^{-1}\,. \tag{23}$$

(We ignore the slight complication that x is reduced by a factor $(K+N)/(K+N+1)$ whenever N jumps up; this factor is close to unity for realistic K.)

Qualitatively this example is similar to the previous example, and plots of $P_N(x)$ versus x and N have the same appearance as those shown in Fig. 4 for the simple T cell model. Deterministically, flare-up (in the case of cancer called *relapse*, which follows the transient *remission* due to the drug's effects) is assured, whereas stochastically there is a positive probability of eradication provided the dose given is large enough relative to the present size of the tumour. When decay is relatively fast (large $\mu K/\rho$), the probability of eradication decreases rapidly with tumour size N, whereas the relative effectiveness of the drug (ϑ/ρ) determines how gradual this drop-off in probability is.

Suppose that a clinician wants to know the minimal dose required to assure eradication to within, say, 0.1%. For this information, she might consult a nomogram that charts that relapse probability as a function of tumour size and dose administered. In the present notation amounts to $1-P_N(x)$ for a tumour size N and a dose equivalent to x; such curves are shown in Fig. 5. This shows that, as expected, increasing the dose reduces the relapse probability, but from a certain point onwards further increases in drug dose do not result in further reductions of this relapse probability. The lowest relapse probability that can be achieved depends on the tumour size and the drug's efficacy parameters, in the expected way. This property shows that multiple administrations of the drug will generally be required, but that even when the tumour size is down to a single cell, eradication cannot be assured.

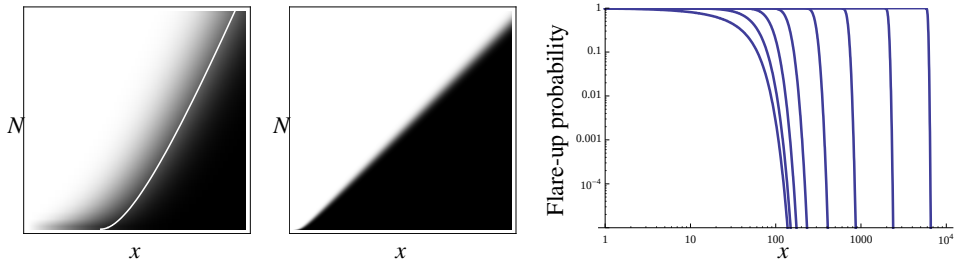

Figure 6: Eradication probability $P_N(x)$ for the T cells with residual surveillance level example (white: probability 0; black: probability 1; grey: probability in interval $(0,1)$). $K = 50$, $\mu = 1$. Left: Abscissa is $0 < x \leq 150$, ordinate is $1 \leq N \leq 30$ (the white line is the deterministic separatrix); middle: $0 < x \leq 2000$, ordinate is $1 \leq N \leq 1000$; right: $1 - P_N(x)$ as a function of x for (top to bottom): $N = 3000$, 1000, 300, 100, 30, 10, 3, 1.

3.3. T cells with residual surveillance level

According to the simple T cell model of Section 3.1, the T cell number decays to zero. However, it has been observed that a small but functionally significant number of antigen-specific T cells remains after the contraction phase: this is the *residual surveillance level* which helps the immune system to suppress re-infection (Harty and Badovinac (2008)). This effect can be explained by the fact that the cytotoxic operation of the T cells tends to damage the T cells themselves as well, so that T cell death is proportional to the rate at which they are themselves destroying infected cells (Xu et al. (2001)). This can be modelled by adjusting the simple model as follows:

$$g \equiv \frac{N}{K+N} \quad h \equiv 1 \quad f = \frac{N}{K+N}$$

On this model specification, the T cells stop dying off as soon as eradication has been achieved.

The deterministic model now has a separatrix, as shown in the right panel of Fig. 1, such that trajectories starting to the right of it terminate in a stationary point on the x-axis, whereas trajectories starting to the left exhibit flare up (i.e. $x \to 0$ and $N \to \infty$ as $t \to \infty$). Thus, in contrast to the previous two examples, the deterministic treatment predicts different values for $P_N(x)$, albeit with $P_N(x) \in \{0,1\}$. As one would expect, the stochastic treatment replaces the abrupt transition about the separatrix by a smooth increase of $P_N(x)$ with increasing x. This is illustrated in Fig. 6, where the separatrix is indicated for comparison. There is a transition region of more or less constant width around the deterministic separatrix (Fig. 6, left and middle panels). For a given size of the infection, the probability of flare-up ($1 - P_N(x)$) falls of rapidly with x once the latter attains a critical level (Fig. 6, right panel). Thus, provided that the immune system expands a sufficiently large clonal response, the probability of flare-up can reliably be reduced to a very small residual level. This can be advanced as an argument in favour of regulated contraction rather than stereotypical, programmed contraction.

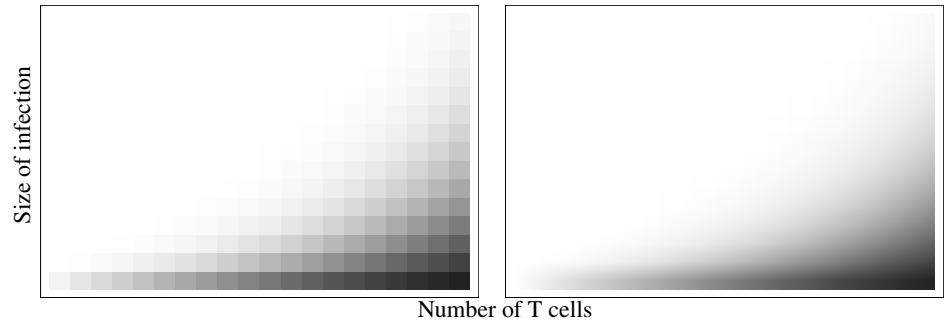

Figure 7: Comparison of fully stochastic (left) and hybrid stochastic-deterministic (right) calculation of $P_N(x)$; $\theta/\rho = 0.05$; $\alpha = 0.01$; $1 \leq X \leq 20$; $1 \leq N \leq 15$ (white: probability 0; black: probability 1; grey: probability in interval $(0,1)$).

3.4. Comparison with a fully stochastic treatment

A fully stochastic treatment becomes necessary when the copy number of the eradicating agents becomes small. Consider the following deterministic model:

$$\frac{d}{dt}X = -\alpha XN \tag{24}$$

$$\frac{d}{dt}N = \rho N - \theta XN \tag{25}$$

where α, ρ, and θ are positive parameters. The eradication probabilities for the stochastic treatment satisfy the following equations by the law of total probability:

$$P_0(0) = 1 \quad \text{and} \quad P_N(0) = 0 \quad \text{for } N \geq 1 \tag{26}$$

$$\rho P_{N+1}(x) - (\rho + X(\alpha+\theta))P_N(x) + \theta X P_{N-1}(x) = -\alpha X P_N(X-1) \quad \text{for } X \geq 1\,. \tag{27}$$

Equation (27) is a non-homogeneous difference equation in N for $P_N(x)$ with x fixed and $P_N(X-1)$ as a forcing term. Thus, by successively solving for $x = 1,2,3,\ldots$ the general solution is readily obtained and found to be:

$$P_N(X) = \sum_{\xi=1}^{X} \binom{X}{\xi} \left(\frac{\alpha\xi}{\rho\,(r_\xi - 1)}\right)^{X-\xi} \kappa_\xi r_\xi^N \tag{28}$$

where

$$r_\xi = \frac{\rho + \xi(\alpha+\theta)}{2\rho}\left(1 - \sqrt{1 - \frac{4\rho\theta\xi}{(\rho+\xi(\alpha+\theta))^2}}\right) \tag{29}$$

and the coefficient κ_ξ is defined by the recursion formula:

$$\kappa_\xi = 1 - \sum_{u=1}^{\xi-1} \binom{\xi}{u} \left(\frac{\alpha u}{\rho\,(r_u - 1)}\right)^{\xi-u} \kappa_u \quad \text{for } \xi \geq 2 \tag{30}$$

with $\kappa_1 = 1$. The results shown in Fig. 7 suggest that even at low values of x, the hybrid approach can give reasonable results.

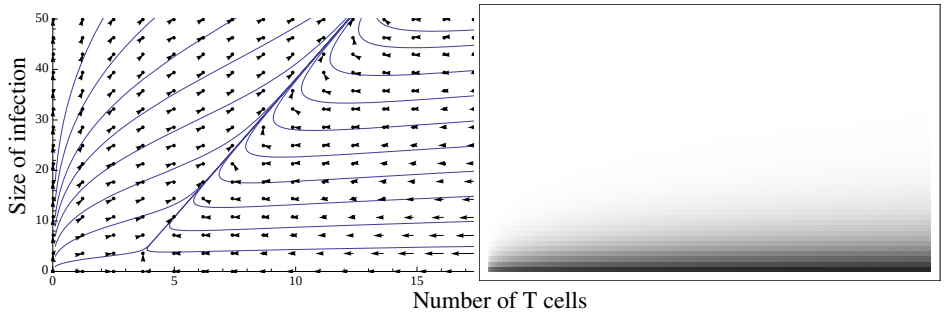

Figure 8: Non-monotone T cell dynamics model for the case $\vartheta\lambda < K$. Left panel: deterministic phase portrait; right panel: probability of eradication from various starting positions (white: probability 0; black: probability 1; grey: probability in interval $(0,1)$).

4. Extension to dynamics with recovery of the eradicating agent

In the foregoing sections it was assumed that the eradicating agent (x) decays monotonically. However, in many systems an adaptive response to the flare-up may occur, where the eradicating agent is added or proliferates in response to the pathogen's escape. By way of example we consider here the following, slightly more complex model of the dynamics of a T cell response:

$$\frac{d}{dt}x = \lambda x - \mu\left(1 - \frac{N}{K+N}\right)x^2 \tag{31}$$

$$\frac{d}{dt}N = \rho N - \vartheta\frac{N}{K+N}x \tag{32}$$

where the T cells x grow with specific growth rate λ whereas they disappear by mutual killing in proportion to the complement of the functional response function (Kottilil et al. (2001); Strasser and Pellegrini (2004); Xu et al. (2001)), which is the usual hyperbolic response (see Van den Berg and Kiselev (2004) for further details on this model). The qualitative behaviour is very different depending on parameter values; when $\vartheta\lambda < K$, the T cells are ultimately unable to stem the spread of the infection (Fig. 8), whereas for $\vartheta\lambda > K$, eradication is assured (Fig. 9). The case $\vartheta\lambda = K$, while interesting in its own right, is not germane to the present discussion.

4.1. The case $\vartheta\lambda < K$

In qualitative terms, the behaviour for $\vartheta\lambda < K$ is somewhat similar to that in the examples of sections 3.1 and 3.2. The eradication probabilities drop off very sharply with increasing N as trajectories become almost certain to converge on a common escape path in the middle of the phase plane (Fig. 8).

Numerical solution of the probability flow equation (9) is slightly more involved. First, the line $x = \delta x$ no longer provides a boundary condition; repeating the argument leading to eqn. (11), we now have

$$P_N(1) = \frac{\rho hNP_{N+1}(1) + \lambda P_N(2) + \vartheta f P_{N-1}(1)}{\rho hN + \lambda + \vartheta f} \tag{33}$$

where we have set $g = 0$ for $N = 1$ since it takes at least two T cells for mutual destruction. Since eqn. (33) uncouples $P_N(1)$ from $P_N(0)$ ($\equiv 0$), a jump discontinuity is admissible. The second difficulty is that the flow

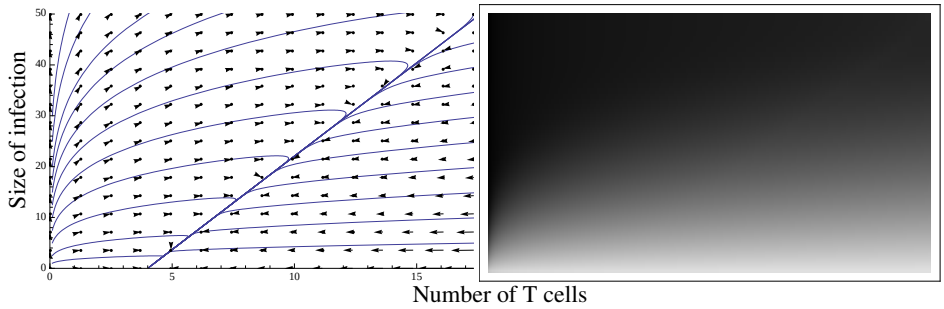

Figure 9: Non-monotone T cell dynamics model for the case $\vartheta\lambda > K$. Left panel: deterministic phase portrait; right panel: expected time until eradication from various starting positions (white: zero time; black: long time).

equations are numerically stable in the positive x-direction for (x,N) situated to the right of $N = (\vartheta/\rho)x - K$ (part of the x null isocline) whereas they are stable in the negative x-direction for (x,N) to the left of this line. Moreover, the equations become infinitely stiff near this line. A Picard iteration scheme (Hirsch et al. (2004)) was employed to obtain the solution shown in Fig. 8 (right panel): numerical solutions are generated alternately for the field above and below the nullcline diagonal, each round of the iteration using the solutions on the other side of the nullcline as forcing functions, starting a distance δx away from the line to avoid the infinite stiffness (since the stiffness amounts to infinitely rapid equilibration between solutions for adjacent N-values, a very fast relaxation rate nearby achieves practically the same effect). The iteration results in a set of values for $P_N(x)$ on the nullcline which serve as consistent boundary conditions for the "forward" and "backward" solutions; in this respect the iterative scheme resembles the shooting technique for nonlinear problems (Burden and Faires (1989)).

4.2. The case $\vartheta\lambda > K$

We noted in Section 2 that $P_N(x) \equiv 1$ for $x > 0$ and $N \geq 1$ solves the probability flow equations, but that the jump discontinuity at $x = 0$ is not allowed by the behaviour near the line $x = 0$. By the argument of Section 4.1, this jump discontinuity is now allowed, and thus $P_N(x) \equiv 1$ is a feasible solution. In the appendix we show that this solution applies when $\vartheta\lambda > K$. Thus, eradication is certain from all starting positions if the immune efficiency parameters are sufficiently large (although eradication may only be achieved through a series of intermediate flare-ups that are ultimately contained). Instead of P_N (a plot of which would not be informative), we consider the expected time until eradication. Thus, let $T_N(x)$ denote the expected time until eradication starting from position (x,N). The derivation is similar; the probability conservation equation (7) now becomes:

$$T(z,N) \doteq \left(1 - \frac{\rho h(z^{-1},N)N + \vartheta f(z^{-1},N)z^{-1}}{\mu g(z^{-1},N)z}\delta z\right) T(z+\delta z,N) + \left(\mu g(z^{-1},N)z + \frac{\rho h(z^{-1},N)N}{\mu g(z^{-1},N)z} T(z+\delta z,N+1) + \frac{\vartheta f(z^{-1},N)z^{-1}}{\mu g(z^{-1},N)z} T(z+\delta z,N-1)\right)\delta z\,. \quad (34)$$

Again, the Picard iteration scheme was used to obtain the results shown in Fig. 9, which suggests that the expected time till eradication is approximately conserved along the fast-moving parts of the deterministic trajectories, as is not surprising. Along the slow moving return trajectory the expected time increases in the

opposite direction of the phase flow, which is partly due to the deterministic travel time along this trajectory and partly due to the possibility of a quasi-flare-up that will ultimately be contained.

5. Concluding remarks

Hybrid stochastic-deterministic dynamical systems constitute a natural approach, since biological systems are almost invariably essentially stochastic, and one should expect the high-numbers justification for a deterministic treatment to be satisfied for some subset of the system's components. The usual deterministic treatment is then seen as a only a special case of the general situation which is a partitioning into a low-numbers component is to be treated stochastically and the high-numbers component can treated deterministically (Kiehl et al. (2004); Wilkinson (2006)). Simulation of such hybrid systems is perfectly straightforward (Alfonsi et al. (2005)); since the hazard rates generally co-depend on the deterministic component, it is necessary to integrate this time-varying hazard in order to realise the time till the next transition in the stochastic component (this time interval being a random variable).

We focussed on rather simplified biomedical examples of eradication-decay dynamics; other examples may be found in pest control, epidemiology, and pharmacodynamics. The key quantity of interest is the probability of eradication (or its complement, the risk of flare-up) starting from a given quantity of eradicating agents. In T cell dynamics, this quantity is the maximal expansion of the responding clonotype; in oncology, it is the dose of drug administered. In both cases, dynamics may be considerably more complicated. Also, probability of flare-up is not the only clinical outcome marker (although it is an important one); the drug administration regime may be chosen to minimise a cost functional that takes into account the hazard rates for various morbidities associated with the tumour mass as well as the drug itself (side effects). To calculate the optimal drug dosage in this case requires an optimal-control approach, such as the one taken in Van den Berg and Kiselev (2004).

Acknowledgement. The authors express their gratitude to an anonymous reviewer for providing insightful comments and suggestions.

Alfonsi, A., Cancès, E., Turinici, G., Di Ventura, B., Huisinga, W., 2005. Adaptive simulation of hybrid stochastic and deterministc models for biochemical systems. ESAIM: Proceedings, 1–10.

Araujo, R. P., McElwain, D. L., 2004. A history of the study of solid tumour growth: The contribution of mathematical modelling. Bull. Math. Biol. 66 (5), 1039–1091.

Badovinac, V. P., Harty, J. T., 2006. Programming, demarcating, and manipulating $CD8^+$ T-cell memory. Immunological Reviews 211, 67–80.

Badovinac, V. P., Porter, B. B., Harty, J. T., 2002. Programmed contraction of $CD8^+$ T cells after infection. Nature Immunol. 3, 619 – 626.

Bargou, R., Leo, E., Zugmaier, G., Klinger, M., Goebeler, M., Knop, S., Noppeney, R., Viardot, A., Hess, G., Schuler, M., Einsele, H., Brandl, C., Wolf, A., Kirchinger, P., Klappers, P., Schmidt, M., Riethmüller, G., Reinhardt, C., Baeuerle, P. A., Kufer, P., 2008. Tumor regression in cancer patients by very low doses of a T cell–engaging antibody. Science 321, 974–977.

Berg, H. A. van den, Kiselev, Y. N., 2004. Expansion and contraction of the cytotoxic T lymphocyte response—an optimal control approach. Bull. Math. Biol. 66, 1345 – 1369.

Burden, R. L., Faires, J. D., 1989. Numerical Analysis, 4th Edition. PWS-Kent Publishing Company, Boston.

de Pillis, L. G., Radunskaya, A. E., Wiseman, C. L., 2005. A validated mathematical model of cell-mediated immune response to tumor growth. Cancer Research 65, 7950–7958.

Harty, J. T., Badovinac, V. P., 2008. Shaping and reshaping CD^+ T-cell memory. Nature Rev. Immunol. 8, 107–119.

Hirsch, M. W., Smale, S., Devaney, R. L., 2004. Differential Equations, Dynamical Systems, and an Introduction to Chaos. Elsevier.

Hudis, C. A., 2007. Trastuzumab — Mechanism of action and use in clinical practice. New Engl. J. Med. 357, 39–51.

Karlin, S., Taylor, H. M., 1975. A First Course in Stochastic Processes, 2nd Edition. Academic Press.

Kiehl, T. R., Mattheyses, R. M., Simmons, M. K., 2004. Hybrid simulation of cellular behavior. Bioinformatics 20, 316–322.

Kottilil, S., Bowmer, M. I., Trahey, J., Howley, C., Gamberga, J., Granta, M. D., 2001. Fas/FasL-independent activation-induced cell death of T lymphocytes from HIV-infected individuals occurs without DNA fragmentation. Cell. Immunol. 214, 1–11.

Löffler, A., Kufer, P., Lutterbüse, R., Zettl, F., Daniel, P. T., Schwenkenbecher, J. M., Riethmüller, G., Dörken, B., Bargou, R. C., 2000. A recombinant bispecific single-chain antibody, CD19 $\times$ CD3, induces rapid and high lymphoma-directed cytotoxicity by unstimulated T lymphocytes. Blood 95, 2098–2103.

Melero, I., Hervas-Stubbs, S., Glennie, M., Pardoll, D. M., Chen, L., 2007. Immunostimulatory monoclonal antibodies for cancer therapy. Nature Rev. Cancer 7, 95–106.

Sachs, R. K., Hlatky, L., 2010. A rapid-mutation approximation for cell population dynamics. Bull. Math. Biol. 72 (2), 359–374.

Strasser, A., Pellegrini, M., 2004. T-lymphocyte death during shutdown of an immune response. TRENDS Immunol. 25, 610–615.

Wilkinson, D. J., 2006. Stochastic Modelling for Systems Biology. Chapman and Hall.

Xu, X.-N., Purbhoo, M. A., Chen, N., Mongkolsapaya, J., Cox, J. H., Meier, U.-C., Tafuro, S., Dunbar, P. R., Sewell, A. K., Hourigan, C. S., Appay, V., Cerundolo, V., Burrows, S. R., McMichael, A. J., Screaton, G. R., 2001. A novel approach to antigen-specific deletion of CTL with minimal cellular activation using $\alpha 3$ domain mutants of MHC class I/peptide complex. Immunity 14, 591–602.

Appendix: Eradication probabilities for the non-monotone T cell dynamics model

We consider the system

$$\frac{d}{dt}x = \lambda x - \left(1 - \frac{N}{K+N}\right)x^2 \tag{.1}$$

$$\frac{d}{dt}N = N - \vartheta\frac{N}{K+N}x \tag{.2}$$

which is a scaled version of the system defined by equations (31) and (32). Deterministically, the stationary point $(x,N) = (\lambda, 0)$ is a global attractor if $\vartheta\lambda > K$, whereas stochastically, flare-ups may occur, but eventual eradication is assured. To prove this, let $\mathscr{R}$ denote the region

$$\mathscr{R} \stackrel{\text{def}}{=} \left\{(x,N) \mid x > \lambda \;\&\; 0 < N \leq K\left(\frac{x}{\lambda} - 1\right)\right\}$$

and define

$$\widetilde{N}(x) \stackrel{\text{def}}{=} \text{ent}\left(K\left(\frac{x}{\lambda} - 1\right)\right) \tag{.3}$$

where ent$(\cdot)$ is the entier function $\mathbb{R} \to \mathbb{N}$ which rounds its argument down to the nearest integer. Suppose that every trajectory must eventually (re)visit $\mathscr{R}$. Since the downward jump probabilities are strictly positive, the probability that the phase point, starting from $\widetilde{N}(x)$ for some finite x, on its next exit from $\mathscr{R}$ does so by eradication (i.e. absorption to $N = 0$) is bounded away from zero. Furthermore, since x is monotonically decreasing for phase points in $\mathscr{R}$, a trajectory traversing $\mathscr{R}$ must eventually exit $\mathscr{R}$, either by eradication or into the region where $N > \widetilde{N}(x)$. Therefore the probability that a trajectory starting from an arbitrary point (x,N) with $x > 0$, $N > 0$ will exhibit n exits from $\mathscr{R}$ without eradication is bounded above by $(1-\delta)^n$ for some $\delta > 0$. Since this probability tends to zero as $n \to \infty$, every trajectory must eventually exit $\mathscr{R}$ by eradication.

It remains to show that every trajectory must enter $\mathscr{R}$. Consider a trajectory starting from a phase point outside of $\mathscr{R}$, and let $u_N(x)$ denote the probability of absorption into $\mathscr{R}$ starting from the point (x,N). Also, let $v_{N-\widetilde{N}(x)}(x)$ denote this probability when x is held fixed. Since clearly $u_N(x) = 1$, we have $v_0(x) = 1$. Suppose that the trajectory never enters $\mathscr{R}$. Along such a trajectory, x increases monotonically, either without bound or, if N remains constant from some point in time onwards, bounded by a finite value. However, the latter possibility is ruled out since the jump probabilities are nonzero. Thus x must tend to infinity along a trajectory that never enters $\mathscr{R}$. This fact, together with the dependence of the jump probabilities on x, implies that $u_N(x) \geq v_{N-\widetilde{N}(x)}(x)$. It therefore suffices to show that $v_{N-\widetilde{N}(x)}(x) \to 1$ for all $N \geq 1$ as $x \to \infty$. This is the case precisely when the following quantity diverges:

$$S(x) \stackrel{\text{def}}{=} \sum_{i=1}^{\infty}\left(\prod_{j=1}^{i}\frac{\vartheta x}{K + \widetilde{N}(x) + j}\right) \tag{.4}$$

(see e.g. (Karlin and Taylor, 1975, p. 147)). To establish this divergence, let $m(x)$ be a function $\mathbb{R} \to \mathbb{N}$ such that

$$m(x) < \vartheta x - \widetilde{N}(x) - K \quad \text{and} \quad \begin{cases} m(x) \to \infty \\ m(x)/x \to 0 \end{cases} \quad \text{as } x \to \infty$$

and let

$$r(x) \stackrel{\text{def}}{=} \widetilde{N}(x) - K\left(\frac{x}{\lambda} - 1\right). \tag{.5}$$

By definition, $0 \leq r(x) < 1$ and thus $\lim_{x\to\infty} r(x)/x = 0$. The sum $S(x)$ can be bounded below by a geometric sum:

$$S(x) \geq \sum_{i=1}^{\infty} \left(\prod_{j=1}^{i} \frac{\vartheta x}{K + \widetilde{N}(x) + i} \right) = \sum_{i=1}^{\infty} \left(\frac{\vartheta x}{K + \widetilde{N}(x) + i} \right)^{i} \geq \sum_{i=1}^{m(x)} \left(\frac{\vartheta x}{K + \widetilde{N}(x) + i} \right)^{i} \geq \sum_{i=1}^{m(x)} \left(\frac{\vartheta x}{K + \widetilde{N}(x) + m(x)} \right)^{i}$$

$$= \frac{\vartheta\lambda}{\vartheta\lambda - K - \lambda(m(x) + r(x))/x} \left(\left[\frac{\vartheta\lambda}{K + \lambda(m(x) + r(x))/x} \right]^{m(x)} - 1 \right) \quad (.6)$$

which diverges as $x \to \infty$ when $\vartheta\lambda > K$.